

*Revised version uploaded to Science Feb 20, 2008*

**Fracture Propagation to the Base of the Greenland Ice Sheet During Supraglacial Lake Drainage**

Sarah B. Das<sup>1</sup>, Ian Joughin<sup>2</sup>, Mark D. Behn<sup>1</sup>, Ian M. Howat<sup>2</sup>, Matt A. King<sup>3</sup>, Dan Lizarralde<sup>1</sup>, Maya P. Bhatia<sup>4</sup>

<sup>1</sup> Department of Geology and Geophysics, Woods Hole Oceanographic Institute, Woods Hole, MA 02543, USA

<sup>2</sup> Polar Science Center, Applied Physics Lab, University of Washington, 1013 NE 40th St., Seattle, WA 98105-6698, USA

<sup>3</sup> School of Civil Engineering and Geosciences, Newcastle University, Newcastle upon Tyne, NE1 7RU, UK

<sup>4</sup> Department of Geology and Geophysics, MIT/WHOI Joint Program, Woods Hole, MA 02543, USA

**Surface meltwater that reaches the base of an ice sheet creates a mechanism for the rapid response of ice flow to climate change. The process whereby such a pathway is created through thick, cold ice has not, however, been previously observed. We describe the rapid (<2 hours) drainage of a large supraglacial lake down 980 m through to the bed of the Greenland Ice Sheet initiated by water-driven fracture propagation evolving into moulin flow. Drainage coincided with increased seismicity, transient acceleration, ice sheet uplift and horizontal displacement. Subsidence and deceleration occurred over the following 24 hours. The short-lived dynamic response suggests an efficient drainage system dispersed the meltwater subglacially. The integrated effect of multiple lake drainages could explain the observed net regional summer ice speedup (1).**

The Greenland Ice Sheet flows outward from its interior through a combination of internal deformation and basal sliding, losing mass around its edges through melt-water runoff and iceberg calving. Recent observations show that ice flow along the western margin accelerates during the summer when surface meltwater lubricates sliding at the ice-bedrock interface (1, 2). Aside from theoretical predictions (3-5) and observations on small icecaps (6), it has not been established how surface meltwater penetrates through thick, subfreezing ice (7, 8). Ice-sheet models used to predict future sea level-rise typically do not include the impact of surface meltwater on ice dynamics. Attempts to include the effects of enhanced basal lubrication within these models suggest increased meltwater may substantially accelerate ice sheet mass loss, but confidence in these results is limited by a poor understanding of ice sheet hydrology (9). Key unknowns in

determining Greenland's potential response to climate forcing are the timescales and pathways through which meltwater reaches the ice sheet's base and its consequent effect on basal motion (10).

For surface meltwater to reach the bed a through-ice conduit is required. Theoretical models of fracture propagation through ice suggest that once initiated, water-filled crevasses will propagate rapidly downward through the full ice thickness to the bed (3-5). In such models the rate of crack propagation is limited only by the meltwater supply needed to keep the crack full (3, 4). Supraglacial lakes (11-13) can provide the large volumes of water required to propagate fractures to the bed (7), thus these lakes are likely critical for establishing a through-ice conduit (moulin). Furthermore, moulins that form in lake basins lie near the confluence of meltwater streams and will continue to be supplied with surface meltwater after the lake drains, routing water to the bed and delaying closure while sufficient meltwater production continues throughout the summer.

To investigate lake drainage and the ensuing ice-sheet response, we established study sites at two large (2+ km diameter) lakes on the ice sheet's western margin at locations with thick (~980 m) (14), subfreezing ice (15). During July 2006, our northernmost study lake (68.72°N, -49.50°W) drained rapidly in an event captured by local GPS, seismic and water-level sensors (Fig. 1) (16). A similar, although less well documented, drainage event occurred at this lake again in 2007 (Fig. S1).

The lake began filling in early July 2006 reaching its maximum extent around 00:00 (UTC) on July 29, 2006, with a surface area of 5.6 km<sup>2</sup> and a volume of  $0.044 \pm 0.01$  km<sup>3</sup>

(16). The lake level then began to fall slowly and steadily at 1.5 cm/hour. At approximately 16:00 UTC the same day, the lake level began dropping rapidly, reaching a maximum drop rate of 12 m/hr between 16:40 and 17:00 (Fig. 2). Extrapolation of the depth-logger data (Fig. 2) indicates the entire lake drained in ~1.4-hours. The average drainage rate ( $8700 \text{ m}^3/\text{s}$ ) during this rapid-drainage phase exceeded the average flow rate over Niagara Falls.

Local vertical and horizontal movement of the ice sheet occurred coincident with the lake drainage. A GPS station located ~0.5 km north of the lake (Fig. 1) recorded both rapid uplift (1.2 m) and northward horizontal motion (0.8 m) with the maximum surface displacement occurring between 17:15 and 17:30 UTC (Fig 2). This northward motion was significantly faster and orthogonal to the mean westerly velocity of 93 m/yr . The following 24 hr period was characterized by gradual subsidence and return to the mean westerly motion accompanied by a transient speedup in the downflow direction. In total, the event resulted in a net westerly surface displacement of 0.5 m in excess of the average daily displacement of 0.25 m (Fig. 2c and Fig. S2.)

A seismometer located ~0.7 km north of the lake (Fig. 1) recorded elevated activity beginning around 15:30 UTC, ~30 minutes prior to the period of rapid lake drainage. The maximum amplitude in seismic energy occurred between 16:45 and 18:00 UTC, during and slightly after the period of rapid lake drainage (Fig S3).

Site visits provided observations of pre-drainage (July 2006) and post-drainage (July 2007) surface features. We found several km-scale fractures running through the lake

basin in 2007. Many were closed at depth (water filled) and no longer draining. Two large moulins were found along the fractures, actively draining the area in 2007 (Fig. 1). A dominant topographic feature in 2007 was an up-lifted section of the ice sheet roughly centered over the lake bottom, forming a flat-topped block of ice ~6 m high and 750-m wide (Fig. 1). This block likely was uplifted as water was rapidly injected to the base of the ice sheet near the lake's center during the 2006 drainage event (16). The block's southern edge lay along a ~3.2 km fracture visible from the air and in synthetic aperture radar (SAR) imagery spanning the lake basin's full width; the northern edge lay along a similarly visible fracture (Fig. 1).

The observed fractures and rapid drainage, synchronous with uplift and horizontal acceleration, are strong evidence that water-driven fracture propagation likely established a hydrological connection to the bed. These observations suggest that hydrologic connectivity occurs in four stages: slow initial drainage; connection to the bed and rapid lake drainage through an extensive fracture system; moulin formation and closure of fractures; and subsequent moulin-routed drainage of daily surface melt to the ice-sheet bed.

The 16-hour initial drainage stage was characterized by a slow, steady drop in lake level, elevated seismicity in the 30 minutes prior to rapid drainage (Fig. S3), and little to no acceleration or uplift at the GPS site (Fig. 2). This initial phase may have coincided with water-filled fracture propagation beneath the lake through the kilometer-thick ice. The main crack's 3.2 km length (Fig. 1) could have stored a volume of water

corresponding to the initial lake-level drop, assuming a 0.5-m wide average opening. Alternatively, the pre-drainage may have started as the lake began spilling over a low drainage divide where the main fracture intersects the western shoreline, filling an existing dry crack at the lake edge so that it hydro-fractured into and through the ice beneath the lake. Surface strain-rates from satellite derived velocities (1) are tensile ( $\epsilon_{xx} = 0.003 \text{ yr}^{-1}$ ;  $x$  directed along flow) along this western shoreline, favoring crevasse formation, whereas strain rates near the lake's center are compressive ( $\epsilon_{xx} = -0.004 \text{ yr}^{-1}$ ). At neighboring lakes we observed similar situations in which lakes spilled over into shoreline cracks creating moulins. Where the fracturing ran adjacent to rather than through the lake basin, drainage occurred over weeks as over-flow melted and deepened the spillover channel leading to the moulin. For either hypothesis, the low seismicity, lack of uplift and acceleration, and the slow drainage rate suggest that little to no water reached the bed of the ice-sheet during this first stage, .

The second stage began when the fractures breached the full ice-thickness, establishing a direct connection to the basal hydrological system. Rapid lake drainage (1.4 hours) was accompanied by an increase in seismic energy (Fig. S3) and synchronous surface displacement of the adjacent shoreline up (1.2 m) and away (0.8 m) from the lake center (Fig. 2). The short duration between the drop in lake level and shore-based surface motion indicates rapid and direct transport of water to the bed. Uplift at the center of the lake was likely larger than the 1.2 m observed nearby on shore, and probably coincided with uplift of the large block at the lake's center. The synchronous uplift indicates a nearly vertical path to the bed, as well as the formation of a transient subglacial lake

which displaced the overlying ice. The high drainage rate and the presence of rafted ice blocks observed along lake-bed fractures suggest that drainage occurred along most of the fractures' length. The turbulent water flow during the rapid discharge would have melted the fracture walls through frictional heating, concentrating flow-paths and leading to the development of larger diameter openings at points where inflow was greatest (6). During the third stage, which lasted a few days following the rapid lake drainage, we hypothesize that most of the fractures closed at depth and discrete moulins formed. The surface water flow ( $\sim 24 \text{ m}^3/\text{s}$ ) previously filling the lake provided inflow into the areas still connected to the bed. Melt widening at locations where inflow was the greatest (e.g., at the ends of surface streams), competing with the tendency of overburden pressure to close the no longer water-filled fractures probably produced and maintained a few discrete moulins that remained open throughout the remainder of the melt season (fourth stage), similar to those we observed post-drainage in 2007 (Fig 1.)

Also during the third stage, the transient subglacial lake drained over a  $\sim 24$  hour period as suggested by the GPS-measured vertical subsidence and horizontal southward motion (Figs. 2 and S2). The relatively rapid subglacial lake drainage suggests the presence of an efficient subglacial hydrological system. Increased ice fracturing likely occurred during this stage as well, possibly explaining the elevated seismic energy in the 1 hour period immediately following the lake drainage (Fig. S3).

Throughout the melt season the on-shore GPS recorded fluctuations in ice-sheet velocity of 50–100% that correlate well with calculations of daily melt intensity and

regional ice-sheet flow ( $I$ ). Other than the ~24-hour period following the drainage (Figs. 2 and S2), the character of the pre- and post-drainage speed fluctuations did not differ appreciably ( $I$ ). Thus, the opening of a new moulin draining a large daily melt volume ( $24 \text{ m}^3/\text{s}$ ) had little apparent lasting effect on the local ice-sheet velocity. Instead, we hypothesize this event contributed to the collective formation of a network of regionally-distributed moulins supplying meltwater to the bed that modulated ice flow both before and after the drainage event. Such modulation implies the presence of a well connected subglacial drainage system capable of receiving water inflow at discrete locations and dispersing it uniformly beneath the ice sheet. This creates what appears to be partial ice-bed decoupling associated with a distributed subglacial hydrological system. These indirect observations highlight how much remains to be learned about the subglacial environment beneath the Greenland Ice Sheet.

Our lake drainage observations provide evidence for a fracture-driven process opening a 1-km deep through-ice conduit and injecting a large volume of surface meltwater directly beneath the ice sheet. Although fracturing established the initial connection, additional melting from energy dissipation during the turbulent flow of water in its 1-km descent likely played a role in widening and maintaining discrete moulins that stayed open throughout the remainder of the melt season. Thousands of lakes are formed on the ice sheet's surface throughout the ablation season, and although we have detailed observations from only a single lake, we do not believe the lake drainage we observed was an isolated or unique event. Other Greenland supraglacial lakes have previously been observed to disappear from the surface in one day (12). During ground and aerial



surveys in 2006 and 2007 we investigated over 10 surrounding lake basins near our study site and detected numerous streams draining into moulins across the ice sheet's surface. These systems were observed both where lakes had drained completely and also where lakes cut overflow channels which later drained into nearby fractures and moulins. In addition, all of the post-drainage lake basins that we observed had fractures running across their surface, supporting the fracture-based mechanism for rapid drainage we have described for our study lake. Thus, we have shown that water-driven fracture enabled by the large volume of water stored in supraglacial lakes provides a means by which hydrologic surface-to-bed connections are established through thick ice. Climate warming would lead to earlier and expanded surface lake formation and, as a result, connections to the bed may occur earlier in the melt season and over a larger area, although further work is needed to constrain the limits of this area. This would increase the annual subglacial throughput of meltwater and may substantially impact Greenland Ice Sheet dynamics (1).

## References and Notes

1. I. Joughin *et al.*, *Science* (Submitted).
2. H. J. Zwally *et al.*, *Science* **297**, 218-222 (2002).
3. C. J. van der Veen, *Geophys. Res. Lett.* **34**, L01501 (2007).
4. R. B. Alley, T. K. Dupont, B. R. Parizek, S. Anandakrishnan, in *Annals of Glaciology, Vol 40, 2005*. (Int Glaciological Soc, Cambridge, 2005), vol. 40, pp. 8-14.
5. J. Weertman, *IASH Publ.* **95**, 139-145 (1973).
6. S. Boon, M. Sharp, *Geophys. Res. Lett.* **30**, 1916 (2003).
7. J. L. Bamber, R. B. Alley, I. Joughin, *Earth Planet. Sci. Lett.* **257**, 1-13 (2007).
8. S. J. Marshall, *Earth Planet. Sci. Lett.* **240**, 191-204 (2005).
9. B. R. Parizek, R. B. Alley, *Quat. Sci. Rev.* **23**, 1013-1027 (2004).
10. *IPCC, 2007: Climate Change 2007: The Physical Science Basis. Contribution of Working Group I to the Fourth Assessment Report of the Intergovernmental Panel on Climate Change* (Cambridge University Press, Cambridge and New York, 2007), pp. 996.
11. M. McMillan, P. Nienow, A. Shepherd, T. Benham, A. Sole, *Earth. Planet. Sci. Lett.* **262**, 484-492 (2007).
12. J. E. Box, K. Ski, *J. Glaciol.* **53**, 257-265 (2007).
13. M. Luthje, L. T. Pedersen, N. Reeh, W. Greuell, *J. Glaciol.* **52**, 608-618 (2006).
14. S. Gogineni *et al.*, *J. Geophys. Res.* **106**, 33761-33772 (2001).
15. R. Greve, *J. Clim.* **10**, 901-918 (1997).
16. Methods are available as supporting material on Science Online.

17. Support was provided jointly by NSF and NASA through ARC-0520077 (S.B.D., M.P.B., I.M.H.) and ARC- 520382 (I.J.); The WHOI OCCI and Clark Arctic Research Initiative provided additional support to S.B.D., M.D.B., and D.L.; and a NERC (UK) Research Fellowship supported M.A.K. Logistical and instrumental support was provided by VECO Polar Resources, PASSCAL, and UNAVCO. Early conversations with R.B. Alley helped initiate this project. Comments from two anonymous reviewers substantially improved the content and clarity of the manuscript.

## Supporting Online Material

[www.sciencemag.org](http://www.sciencemag.org)

Methods

Figs. S1

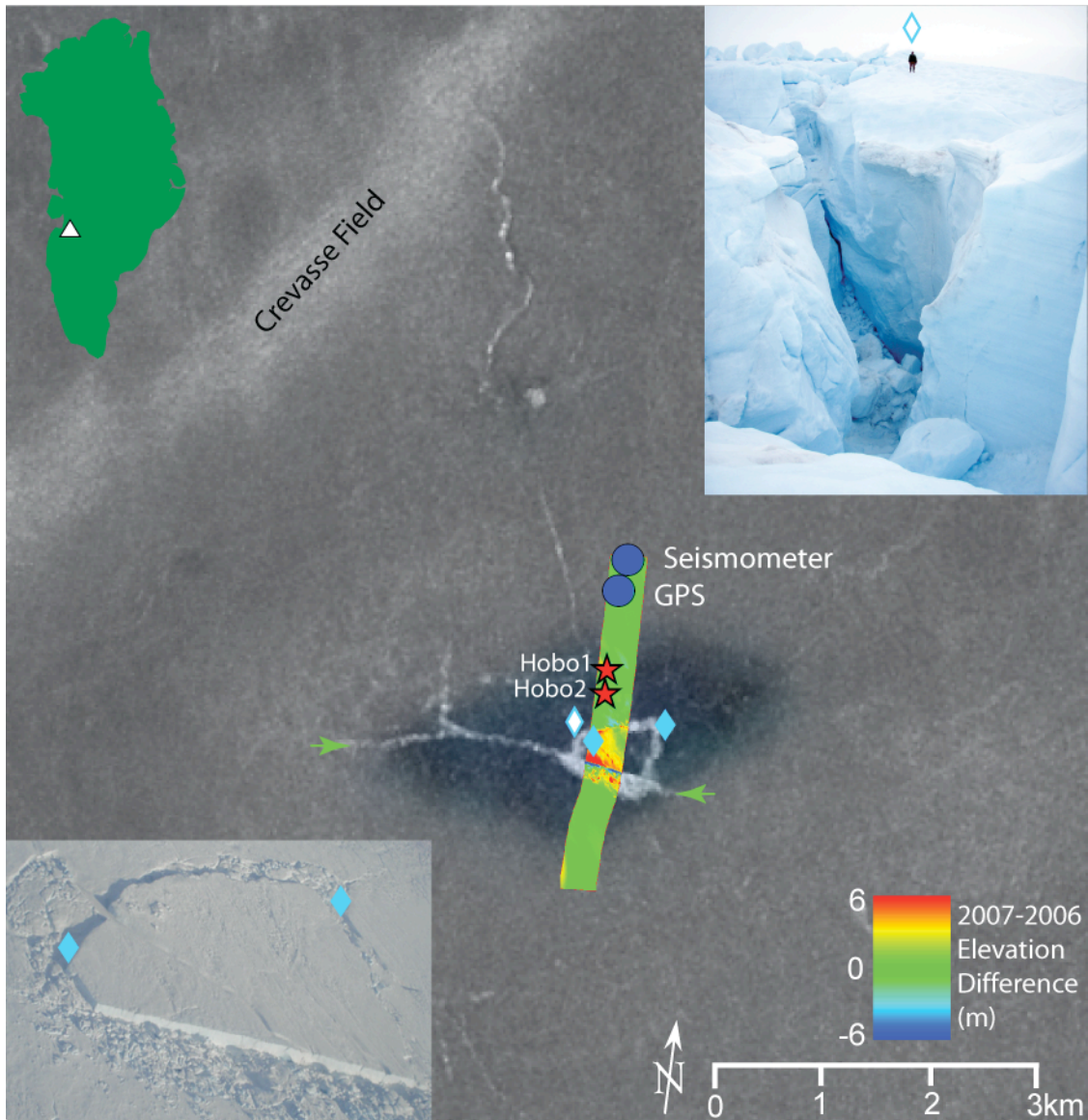


Figure 1. Early October 2006 SAR image (gray scale background) overlaid with a semi-transparent MODIS image showing the lake extent (blue) on July 29, 2006. Red stars show the water-pressure logger locations and blue circles show the GPS/seismometer locations. Block uplift (lower-left inset) is revealed by 2006-to-2007 elevation differences (colored swath) recorded by NASA's Airborne Topographic Mapper (ATM) in May of both years. A large fracture is visible in the SAR image as a long, bright linear feature with ends marked by green arrows. Solid blue diamonds indicate locations where sonar and ATM measurements found large "holes" in the lake bed prior to drainage in 2006. The upper-right inset shows a 1.8 m tall person standing above a similar hole (open blue diamond) located following the 2007 lake drainage.

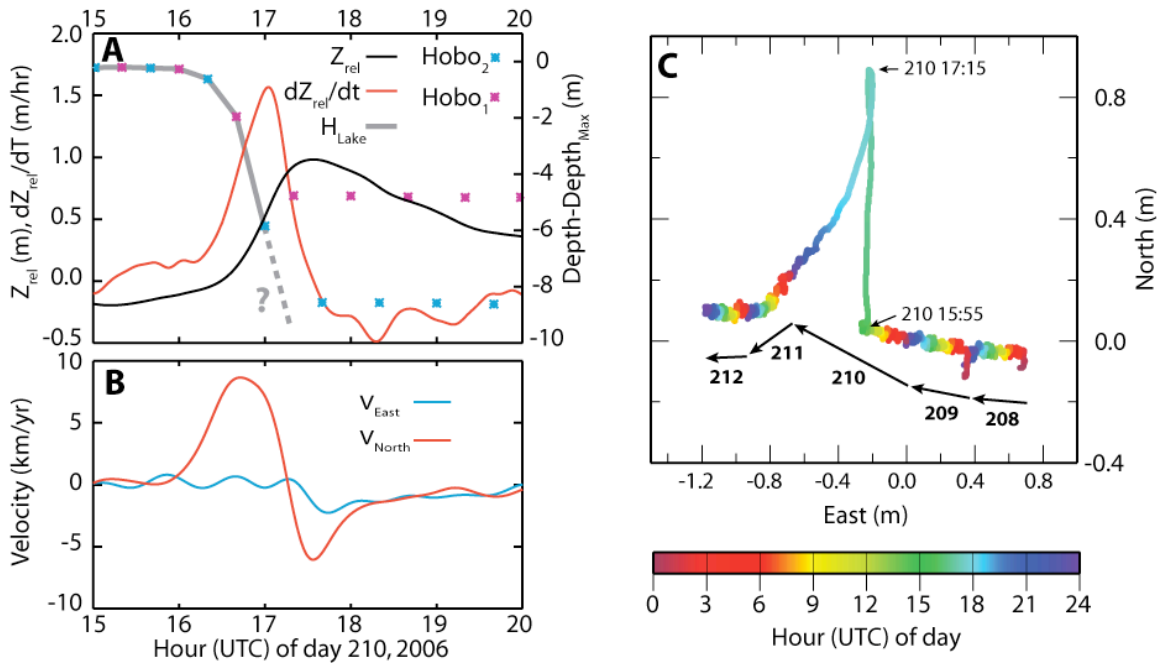


Figure 2. Data from the 2006 lake drainage event. a) Relative elevation and rate of elevation change (left axis: black and red lines respectively) are derived from the on-shore GPS elevations smoothed to 5 minute temporal resolution. Lake level as recorded by water pressure loggers (right axis: blue and purple stars connected with a gray line) and referenced to the lake level just prior to drainage. A linear fit to the last two lake-level measurements when the depth loggers remained submerged suggests the lake drained completely by  $\sim 17:30$  UTC (dashed gray line). b) North (red) and east (blue) velocity components at the GPS station smoothed to 10-minute temporal resolution. c) Relative position of the GPS station during the five days immediately prior to, during, and following the drainage event showing the rapid translation of the surface as it floats up and away from the lake center, and subsequently returns. The color-bar indicates the hour-of-day, while the bold black arrows delineate each day's net motion.

## Supporting Online Material

### Methods and Data

#### *GPS Data*

The continuous GPS data were processed at the full the 15-s resolution using the Track software (1). The data were processed relative to data from a station on bedrock (Kaga), located approximately 55 km from our lake site. In this processing, site motion was constrained on an epoch-by-epoch basis to suppress noise without damping the signal.

#### *Block uplift*

Based on repeated topographic surveys and the timing of GPS surface motion we conclude that the large block in center of the lake (Fig. 1) was uplifted during the lake drainage event in 2006. Sonar surveys of the lake bottom when it was full (July 16, 2006) found no evidence of this feature, although two large, several-meter deep holes were found near the ends of the block's northern edge (Fig. 1). In May 2006 and then again in May 2007, NASA's Airborne Topographic Mapper (ATM) flew over the dry lakebed with its scanning laser altimeter (2). The elevation change between the surveys (Fig. 1) indicates ~6 m of surface uplift across the block. The block also is clearly visible in an ASTER satellite image from August 8, 2006 but not visible in earlier imagery. Together, these sources indicate the uplift occurred sometime between July 16 and August 8, 2006. Other than the lake drainage event, the GPS recorded no other substantial uplift on the nearby shore during this period. Thus, we propose that the large volume of water driven beneath the ice sheet during lake drainage likely produced several meters of uplift at the lake's center concurrent with the meter-scale uplift on the nearby shoreline as recorded by the GPS.

#### *Lake Fill Rate and Volume Calculation*

We had several sources of data for determining lake volume. The first of these was a series of sonar surveys performed by boat on July 16, 2006. We also produced a digital elevation model of the region using a nadir- and backward-looking image pair from July 2005 acquired by the Advanced Spaceborne Thermal Emissivity and Reflection Radiometer (ASTER) aboard the Terra satellite. In RADARSAT SAR images acquired shortly after the lake drained, the area recently covered by water appeared far brighter than the surrounding region, which provided us with an estimate of the lake area near the time of drainage. Finally, we installed two internally logging HOBO pressure transducers at two locations on the lake bottom beginning July 17<sup>th</sup> as well as a third onshore transducer for performing atmospheric pressure corrections to lake level estimates.

We used the DEM to determine the shape of the lake basin, and then adjusted the lake level so that the mean depth agreed with the depths determined by sonar surveys. The standard deviation of the difference between the DEM- and sonar-determined depths was 2.6 m. This procedure gave us an estimated lake volume of 0.019 km<sup>3</sup> and surface

area of  $4.6 \text{ km}^2$  at the time we placed the HOBO loggers in the lake. These instruments measured a  $4.9 \text{ m}$  increase in lake level over the period leading up to the drainage on July 29 (Fig. S2) during which the SAR image indicated the lake area grew to  $5.56 \text{ km}^2$ . Assuming the lake area grew linearly over this period, then the volume increased by  $0.025 \text{ km}^3$  to yield a total volume of  $0.044 \text{ km}^3$  at the time of drainage. Assuming an error in the mean depth of  $1 \text{ m}$  and digitization error of  $125 \text{ m}$  for the boundary, we estimate a volume error of  $0.01 \text{ km}^3$ . Over the period the HOBOS logged data prior to lake drainage, meltwater filled the lake at an average rate of  $24 \text{ m}^3/\text{s}$ .

1. G. Chen, Ph.D., Massachusetts Institute of Technology (1998).
2. W. Krabill *et al.*, *Geophys. Res. Lett.*, **31**, doi:10.1029/2004GL021533 (2004).

## Figures

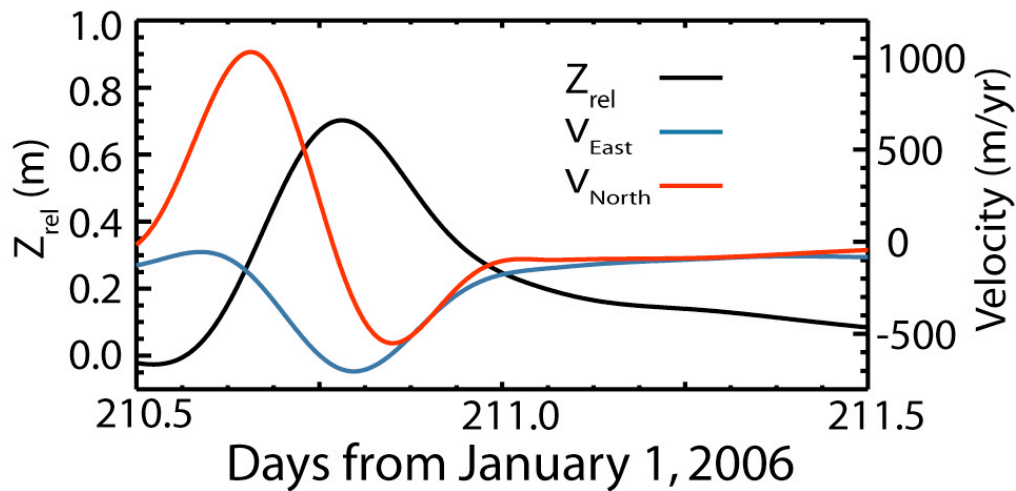


**Figure S1.** Velocity (blue and red lines) and relative elevation (black line) for a 24-hour interval that includes the lake drainage event in 2006. These data are smoothed to 2-hour temporal resolution, which reduces the peak values relative to the higher temporal resolution values shown in Fig. 2.

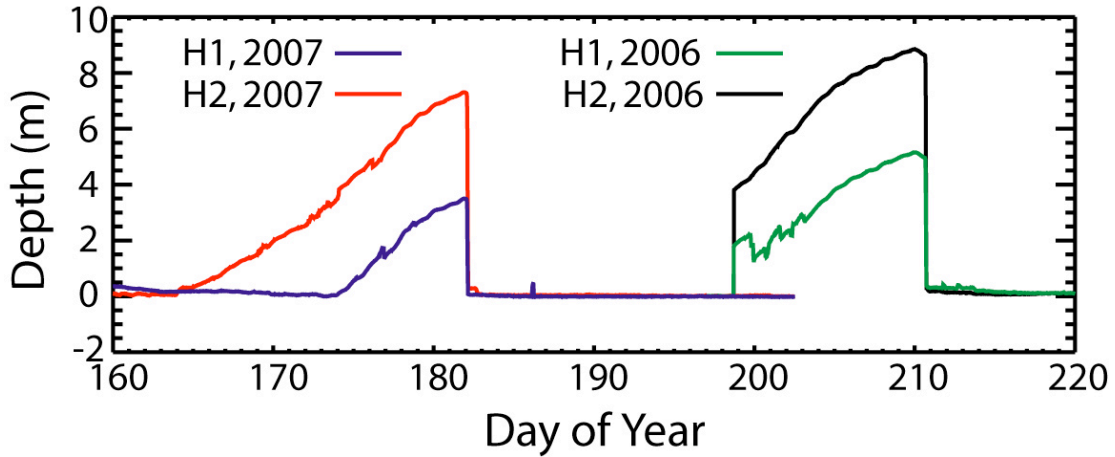


**Figure S2.** Lake depths from the two HOBO pressure transducers showing lake filling (following installation on July 17, 2006) and lake drainage events in 2006 (green and black) and 2007 (blue and red). Depths are corrected for atmospheric pressure using a third HOBO onshore.

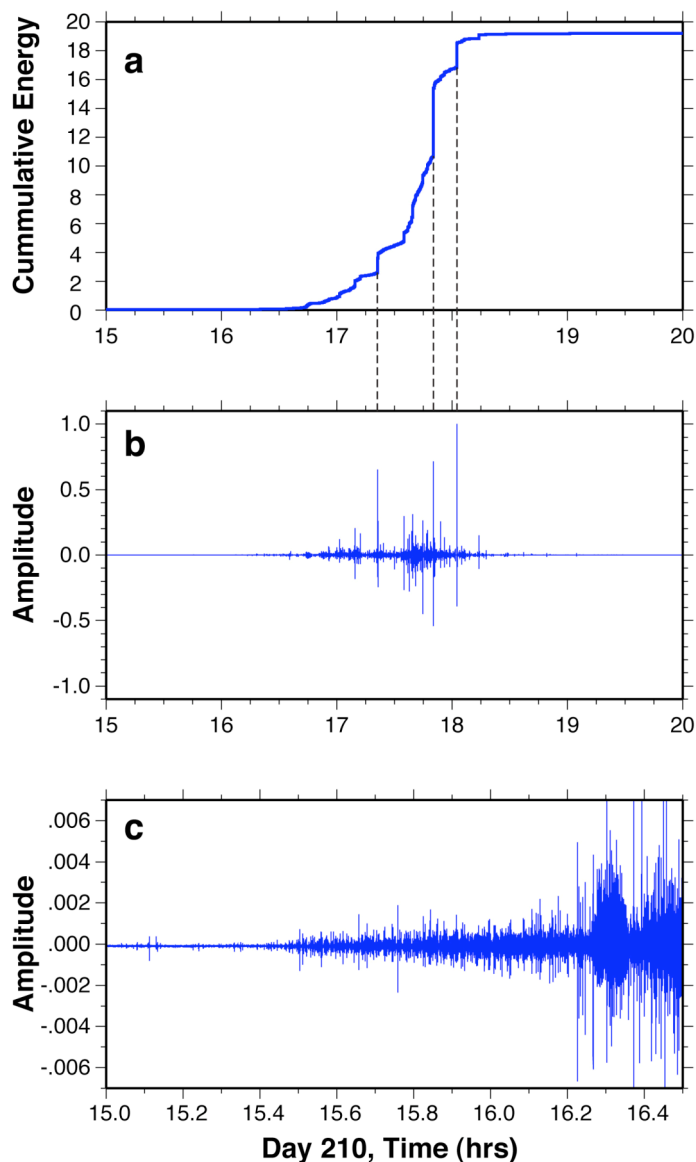


**Figure S3.** Seismic data from day 210 recorded  $\sim 0.7$  km north of the lake, with (a) cumulative energy from the vertical channel from 15:00-20:00 UTC, (b) the vertical-channel trace from 15:00-20:00 UTC, and (c) an enlarged view of the vertical-channel trace from 15:00-16:30 UTC. Cumulative energy is the running sum of the squared, normalized amplitude. This cumulative energy curve summarizes the modes and progression of seismic energy release during the day-210 event.

Seismic energy is observed in two modes, a rumbling mode and a discrete cracking or ice-quake mode. Discrete cracking events release a large amount of energy in a small amount of time and are seen as steps in the cumulative energy curve and as large amplitude deflections in the seismic trace. Prominent



examples are indicated by the dashed lines. It may be possible to relate these cracking events to key events in the evolution of lake drainage, such as the initial crack propagation and the uplift and/or subsequent settling of the central block, but analyses of the seismic data are too preliminary at present to rigorously support such interpretations.

The rumbling mode of energy release is manifest as more or less continuous increases in the cumulative energy curve, with the slope of the curve related to the intensity of the “rumbling”. The initial rapid-drainage phase between 16:00-16:30 UTC is associated with a distinct seismic signal (c) that was seismically quiet relative to subsequent phases of the drainage event. Continuous rapid drainage between 16:30-17:30 UTC was more energetic, yielding a distinct slope in the cumulative energy curve. This slope is offset at ~17:20 UTC by a discrete event that may be related to the central block uplift.

The end of the rapid-drainage phase at ~17:30 UTC is marked by a distinct change in cumulative energy slope, indicating a change to a “noisier” phase of drainage. We speculate that the increased rumbling during this later phase indicates water falling into the now incompletely full crack and ice settling following the period of uplift.